APPLICATIONS OF
MODELLING AND SIMULATION
http://arqiipubl.com/ams eISSN 2600-8084 VOL 8, 2024, 57-69

# Edge Theorem-Based 2-DOF Controller Design for MIMO System

Sumit Kumar Pandey[1*] and Salinda Buyamin[2]

[1]Department of Electrical & Electronics Engineering, Amrita School of Engineering, Coimbatore, Amrita Vishwa Vidyapeetham, 641112, India
[2]Faculty of Electrical Engineering, Universiti Teknologi Malaysia, 81310 UTM Johor Bahru, Johor, Malaysia

*Corresponding author: p_sumitkumar@cb.amrita.edu

*Submitted 02 December 2023, Revised 17 January 2024, Accepted 21 February 2024, Available online 01 March 2024.*


**Abstract:** The designing and implementation of controllers on multiple-input multiple-output (MIMO) plants for achieving a robust performance are always a promising problem for design engineers. Decoupler is one of the vital applied algorithms to minimize the undesirable effect of cross couplings present in MIMO plants for improving the plant performance. However, the inclusion of a decoupler makes the resulting decoupled system more complex, thereby increasing the computational complexity of designing the controller. To enhance performance, this paper aims to design a controller without incorporating any decoupling technique. This approach is intended to make the compensated system effectively track the desired path while treating coupling effects as a disturbance. The two degrees of freedom (2-DOF) proportional integral derivative (PID) control method is employed including a filter coefficient in derivative part based on edge theorem considering the MIMO system as different single-input single-output subsystems on which the cross couplings act as a disturbance to each other. The optimum value of controller parameter is searched in between the range determined through edge theorem using particle swarm optimization technique. The designed controller is implemented to the twin rotor MIMO system in which the designed method is quite capable of minimizing the disturbances occur for the reason of cross coupling. It is seen that in 2-DOF PID control method, the maximum overshoots are found to be 0% and 8% for main and tail rotor, respectively which are superior as compared to the conventional PID controller with decoupler designed for same system where the maximum overshoots are found as 30% for both main and tail rotors. The robust performance of compensated plant is studied by plant parameter variation, output disturbance rejection and changing the nature of input signals to the plant.

Keywords: Edge theorem; MIMO; Particle Swarm Optimization; PID; Twin rotor.

## 1. INTRODUCTION

In this work an innovative approach of controller design is proposed for effective control of multiple-input multiple-output (MIMO) systems even in the presence of disturbances. Unlike conventional methods, this approach does not employ any decoupler algorithm to eliminate coupling effects within the MIMO system. Instead, it treats the coupling effects within the MIMO system as input disturbances to the plant and a 2-degree of freedom (DOF) and PID controller is designed to address this challenge. The 2-DOF control strategy consists of two separate components, ensuring both precise reference tracking and effective disturbance rejection. The study uses a twin rotor MIMO system (TRMS) as an illustrative example of a MIMO system due to its highly nonlinear behavior and strong cross-coupling characteristics [1]. The control approach adopted here represents a fusion of classical and modern control techniques. To elaborate, a classical 2-DOF PID controller is initially designed. However, the parameter ranges for the controller are determined using the edge theorem and subsequently fine-tuned through the particle swarm optimization (PSO) method.

In recent years, robustness design analysis has achieved a remarkable importance. It is a vital area of control techniques that deals mainly with perturbations, disturbances, and model variations for controller design. The control algorithm is formulated to function properly despite the uncertainty attached with the plant. A controller is said to be robust when it maintains its performance regardless of plant modelling errors or disturbances associated with it. PID controllers are widely used for robust control because of their ease of application and tendency to provide accurate results [2-5]. The DOF in control structure is commonly known as how independently the system can vary in different directions. It may be defined as the total count of transfer function in closed loop which can be varied without any dependency. The 1-DOF structure shows limited performance such that it cannot provide good results for both time domain responses and disturbance rejection at the same time which may be obtained with 2-DOF control structure [6-7]. In [8], a 2-DOF Single-Input Single-Output (SISO) control

technique is implemented for decoupled TRMS to get the satisfactory performance of the system. The designed controller also ensured sufficient loop robustness and disturbance rejection properties. Here a pre-compensator is designed to achieve the decoupling of TRMS system. In [9], TRMS is controlled using a particular algorithm known as robust deadbeat algorithm. In this work, performance is tested in terms of robustness for designed controller considering disturbances as the coupling effects. This design method is implemented in simulations as well as real time validation is also done. In [10], coupling effects on the TRMS were minimized by sliding surfaces designed especially for the same purpose. This cross coupling causes the deterioration in the responses during the movement of TRMS and it is minimized as considering the disturbances or externally a decoupling method is introduced to remove this undesired coupling. Particularly for non-linear MIMO plant, sliding mode control (SMC) technique ensures robust performance with respect to coupling effects. Only by being aware of the system's input and output one can use the model reference method of control to assure the robust functioning of MIMO systems [11]. Gain theorem is employed in the design of suitable robust controller, for such type of system where the parameters are not fixed rather it is varied simultaneously. Gain theorem provides the condition for determining the robust stability of polynomials with perturbed coefficients [12]. In [13], PSO-based PID control method is depicted to get the desired performance for TRMS. In [14], SMC sliding mode control method is designed and successfully implemented on TRMS. In [15], robust $H_\infty$ method of control is proposed to get the satisfactory performance of TRMS. The combination of robust sensitivity is described for getting the more accurate performance in respect of reference tracking in this work. In [16], the authors described the tracking performances as well as reducing the vibration control of TRMS due to mass variation. An optimal control using linear quadratic Gaussian method is proposed to get the desired performance from TRMS. In [17], TRMS is controlled by predictive controller based on robust optimal method. The output responses of TRMS were examined using step signal at the input.

PID controller using different optimization methods are applied to control TRMS is discussed in [18-20] and performance with respect to time domain is also compared in this work. The concept of decoupling is applied in this work to reduce the coupling effects present in the system and controller is designed based on decoupled plant. In [21], different control techniques which included PID control, optimal control and nonlinear control techniques were suggested by authors for the control of TRMS. A data driven neuroendocrine PID method was proposed in [22] to control the TRMS. The controller gains are optimized through adaptive safe experimentation dynamics technique. A robust controller based on quantitative feedback theory is designed to control TRMS in [23]. In this work, the stabilization of the plant is guaranteed with improved tracking performance. In [24], quasi-linear parameter varying proportional integral controller is proposed by authors for getting the desired performance of TRMS. The condition of actuator saturation was also considered in this work for the designing of controller. Fractional order PID controller was designed for decoupled TRMS using optimization method in [25]. Comparative study of different control methods using PID control, linear quadratic regulator and linear quadratic Gaussian was discussed in [26]. The modified internal model control method was proposed in [27]. Different MIMO system examples which included square MIMO and no-square MIMO systems were considered in this work. A robust controller was designed in [28] using generalized decoupling method for an unstable MIMO plant. Optimal control technique was applied to stabilize the plant first before designing of controller. The extensive process of literature review revels that the robust controller designed for control of TRMS is mainly executed with the design of decoupler along with controller which also minimize undesired outputs due to interactions present in MIMO system. Incorporation of decoupler during the controller design procedure makes the compensated MIMO system more complicated in view of structure. Therefore, in this work, a controller is applied to the system without incorporating any decoupler assuming the undesired interaction outputs as disturbance.

The main objective of controller design for any system is that the output performance of the compensated system should satisfy the desired criteria and the designed controller is known as robust if the output response remains unchanged while disturbance occurred in plant. PID controller remarkably showed its importance towards the accurate controller design for different types of plants and industrial applications [29-34]. One of the difficult tasks of controller design is to find the range of controller parameters for which systems remain stable. Some methods were suggested in [35] but it makes the calculation tedious that insist the authors in this work to design the robust controller using edge theorem which is comparatively less complicated than the method reported. The performance and efficiency of edge theorem is excellent for the designing of robust controller with guaranteed stability [36-37]. In this work, edge theorem is applied to get the ranges of controller gain values and further to achieve the optimum performance of the controller, PSO method is implemented within the zone found by the aforesaid theorem. The output results exhibit that output performance of plant is better in term of both transient as well as steady state with respect to results available in literature. The subsequent content outlines the substantial contributions made within this paper:

a) The robust controller design for TRMS is carried out without incorporating any decoupling technique to ensure the smooth performance in presence of decoupling also considered as disturbance.
b) Main objective in this work is to design the control method to minimize these coupling effects as well as to ensure the satisfactory time response to ensure the smooth performance. To achieve this, a 2-DOF PID controller with derivative filter coefficient (PIDF) is designed.
c) Robustness criteria of proposed method is also examined through the plant parameter variation and applying different inputs at the same time on the compensated plant.

The paper is narrated in different parts, as Section 2 provides a description of the system and the 2-DOF PID control scheme is stated in Section 3. Section 4 deals with implementation of controller and simulation results for different sets of inputs. Finally, Section 5 consists of conclusion and discussion of this paper.

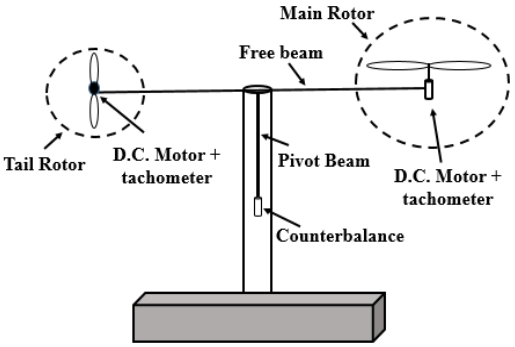


Figure 1. TRMS model.

## 2. MATHEMATICAL MODELLING OF TRMS

It is important to conduct mathematical modelling accurately to design the controller for any plant. The schematic diagram of plant is portrayed in Figure 1 in which two fans are connected at both ends of beam for controlling the position of the plant. DC motors are used to vary the speed of the fans to know the desired position. The main rotor generates the lifting power that enables the perpendicular rotation of beam across the pitch dimension. The beam is turned left or right in yaw direction because of movement of tail rotor, the size of tail rotor is much smaller as compared to previous rotor. Two locking screws are available to physically prevent collision between the two rods in which rotors are mounted. TRMS rotation could be locked in both axes of rotation and any of them using the screw. Therefore, experiments in one and two DOFs can be run on this system. A counterweight that is at the top of rod establishes a reliable starting position of beam.

TRMS is designed in order that it should stay in downward direction always when no supply is provided to the system. TRMS is laboratory prototype test rig which is inherently nonlinear. The equations required to govern the TRMS are derived as in [4]. Firstly, the main (pitch) angle ($\psi$) momentum is calculated through:

$$I_1\dot{\psi} = M_1 - M_{FG} - M_{B\psi} - M_G \tag{1}$$

The total momentum of rotor is denoted as $M_1 = a_1\tau_1^2 + b_1\tau_1$ that is produced due to momentum $\tau_1$. The gravitational momentum is generated by the weight of helicopter as $M_{FG} = M_g \sin\psi$ whereas frictional and gyroscopic momentum is denoted as $M_{B\psi} = B_{1\psi}\dot{\psi} + B_{2\psi}\text{sign}(\dot{\psi})$ and $M_G = K_{gy}M_1\varphi\cos\psi$, respectively. The input voltage to the main motor is related to the momentum through the equation $\tau_1 = (K_1/T_{11}s + T_{10})u_1$. Similarly, one can represent the total momentum developed through the horizontal rotor ($\varphi$).

$$I_1\dot{\varphi} = M_2 - M_{FG} - M_{B\varphi} - M_R \tag{2}$$

In this, total momentum of the rotor is represented as $M_2 = a_2\tau_2^2 + b_2\tau_2$ and frictional momentum as $M_{B\varphi} = B_{1\varphi}\dot{\varphi} + B_{2\varphi}\text{sign}(\dot{\varphi})$. $M_R = \big(K_c(T_{0s}+1)/(T_{ps}+1)\big)\tau_1$ is the cross-reaction momentum and momentum of tail rotor producing the input to the plant as $\tau_2 = (K_2/T_{21}s + T_{20})u_2$. These two equations are linearized considering origin as an operating point and the parameter values are taken from the lab manual of the TRMS provided by Feedback Instruments Ltd. [1,4]. All the symbols used in this work and their corresponding values are tabulated in Table 1. The ensued transfer matrix can be written where $G_{11}(\text{s})$ and $G_{22}(\text{s})$ are the transfer functions of the main and tail rotors respectively. $G_{12}(\text{s})$ and $G_{21}(\text{s})$ are the transfer function of the coupling effects on main and tail rotor, respectively.

$$G(s) = \begin{bmatrix} G_{11}(s) & G_{12}(s) \\ G_{22}(s) & G_{22}(s) \end{bmatrix} = \begin{bmatrix} \dfrac{1.246}{s^3 + 0.9215s^2 + 4.77s + 3.918} & 0 \\ \dfrac{1.482s + 0.4234}{s^4 + 6.33s^3 + 7.07s^2 + 2.08s} & \dfrac{3.6}{s^3 + 6s^2 + 5s} \end{bmatrix} \tag{3}$$

Table 1. Symbols description and values.

| Symbol | Description | Value | Symbol | Description | Value |
|---|---|---|---|---|---|
| $I_1$ | moment of inertia of vertical rotor | $6.8 \times 10^{-2}$ kg.m$^2$ | $B_{2\varphi}$ | Friction momentum | $1 \times 10^{-2}$ Nms/rad |
| $I_2$ | moment of inertia of horizontal rotor | $2.10 \times 10^{-2}$ kg.m$^2$ | $K_{gy}$ | Gyroscopic momentum | 0.05 s/rad |
| $a_1$ | static characteristic | 0.0135 | $K_1$ | Motor 1 gain | 1.1 |
| $a_2$ | static characteristic | 0.0924 | $K_2$ | Motor 2 gain | 0.8 |
| $b_1$ | static characteristic | 0.02 | $T_{11}$ | Motor 1 denominator parameter | 1.1 |

| | | | | | |
|---|---|---|---|---|---|
| $b_2$ | static characteristic | 0.09 | $T_{10}$ | Motor 1 denominator parameter | 1 |
| $m_g$ | gravity momentum | 0.32 N.m | $T_{21}$ | Motor 2 denominator parameter | 1 |
| $\psi$ | Pitch angle (Main rotor) | _ | $T_{20}$ | Motor 2 denominator parameter | 1 |
| $\varphi$ | Yaw angle (Tail rotor) | _ | $T_p$ | Cross reaction momentum parameter | 2 |
| $B_{1\psi}$ | Friction momentum | $6 \times 10^{-3}$ Nms/rad | $T_0$ | Cross reaction momentum parameter | 3.5 |
| $B_{2\psi}$ | Friction momentum | $1 \times 10^{-3}$ Nms/rad | $K_c$ | Cross reaction momentum gain | -0.8 |
| $B_{1\varphi}$ | Friction momentum | $1 \times 10^{-1}$ Nms/rad | | | |

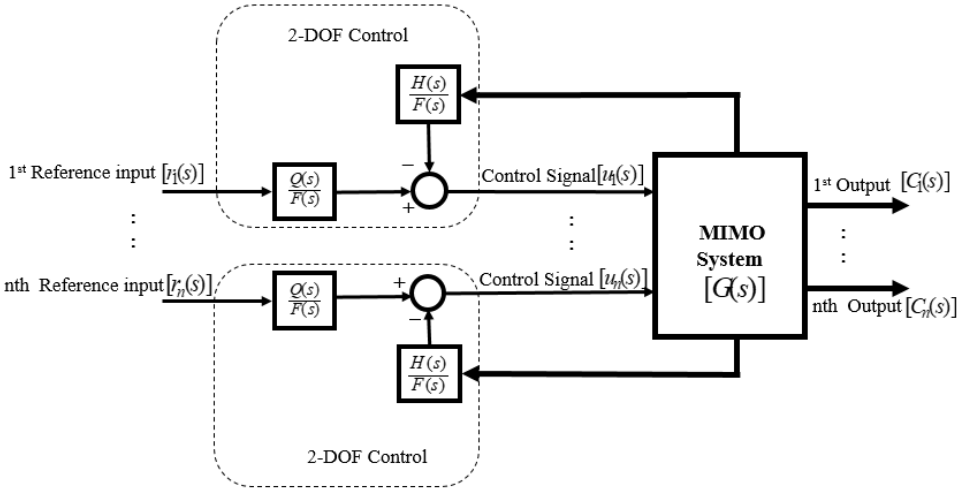


Figure 2. Two degrees of freedom control of MIMO system.

## 3. DESIGN OF CONTROLLER

### 3.1 2-DOF PID structure

In this paper, a 2-DOF based PIDF is proposed based on edge theorem and the 2-DOF control structure is shown in Figure 2. The ranges of parameters of PIDF controller have been obtained based on edge theorem stability criterion and the optimum value of controller parameter has been determined within the obtained range using PSO technique. The structure of 2-DOF controller can be summarized as $H(s)/F(s)$ (feedback controller) and $Q(s)/F(s)$ (feedforward controller) as displayed in Figure 2. $H(s)/F(s)$ is the transfer function of PIDF as in Equation (4) [35],

$$\frac{H(s)}{F(s)} = \frac{K_p s + K_i + K_d s^2}{s(s+N)} \tag{4}$$

where $K_p$, $K_i$ and $K_d$ are proportional, integral, and derivative gains respectively, and $N$ is a filter coefficient. The value of $Q(s)$ is carefully obtained based on pole cancellation so that the transient response of the system become faster [24]. If the transfer functions of TRMS for main and tail rotor are given as

$$G_{11}(s) = (b_{1n}s^n + b_{1(n-1)}s^{n-1} + b_1 s + b_{10})/(s^n + a_{1(n-1)}s^{n-1} + a_1 s + a_{10})$$

and

$$G_{22}(s) = (b_{2n}s^n + b_{2(n-1)}s^{n-1} + b_2 s + b_{20})/(s^n + a_{2(n-1)}s^{n-1} + a_2 s + a_{20}),$$

The closed-loop characteristics equation is formulated in term of coefficient $\delta$ as

$$\delta(s) = s^5 + \delta_4 s^4 + \delta_3 s^3 + \delta_2 s^2 + \delta_1 s + \delta_0 \tag{5}$$

In $Q(s)$, $\alpha$ is calculated in this work as

$$\alpha = \frac{\delta_0}{p_1 p_2 b_{10}} \tag{6}$$

Positions of two poles are $p_1$ and $p_2$ of characteristics equation,

$$Q(s) = \alpha(s + p_1)(s + p_2) \tag{7}$$

### 3.2 Edge Theorem

The stability of the system is a very important aspect of an efficient controller design. For a proper robust controller design, the stability of the system plays a significant role. Any controller is said to be robust when the performance of the system remains unchanged even where there is some change in system parameters or due to disturbances associated with the system. But for testing system stability when precise values are not known, it is quite difficult to test the stability of such a system because the conventional stability techniques are not able to be implemented in such a type of system. To test such stability, a given plant is converted to the interval plants and researchers have shown that the implementation of edge theorem is quite easy as compared to Kharitonov theorem [2-3]. In this method to check the stability of $n$ uncertain parameters $2^n$ polynomials are required. Considering the system whose real numbers are $\alpha_0 < \alpha_1 < \ldots < \alpha_n$ and variable gains are $q = [p_0, p_1, \ldots, p_n]$ in box is $Q = \left\{q: p_i \in [\underline{p_i}, \overline{p_i}], i = 0,1,2,\ldots.n\right\}$. $\underline{p_i}$ and $\overline{p_i}$ are maximum and minimum bounds of $i^{\text{th}}$ perturbation of $p_i$. For $P(s,q)$, $2^{n+1}$ edge polynomials are written as

$$P(s,q) = P_0 s^{\alpha_0} + P_1 s^{\alpha_1} + P_2 s^{\alpha_2} + \ldots. + P_n s^{\alpha_n} \tag{8}$$

$$\begin{aligned} v_1(s) &= \underline{p_0} s^{\alpha_0} + \underline{p_1} s^{\alpha_1} + \underline{p_2} s^{\alpha_2} + \ldots. + \underline{p_n} s^{\alpha_n} \\ v_2(s) &= \overline{p_0} s^{\alpha_0} + \underline{p_1} s^{\alpha_1} + \underline{p_2} s^{\alpha_2} + \ldots. + \underline{p_n} s^{\alpha_n} \\ v_3(s) &= \underline{p_0} s^{\alpha_0} + \underline{p_1} s^{\alpha_1} + \underline{p_2} s^{\alpha_2} + \ldots. + \underline{p_n} s^{\alpha_n} \\ v_{2^{n+1}}(s) &= \overline{p_0} s^{\alpha_0} + \overline{p_1} s^{\alpha_1} + \overline{p_2} s^{\alpha_2} + \ldots. + \overline{p_n} s^{\alpha_n} \end{aligned} \tag{9}$$

The polynomial $P(s,q)$ is said to be stable under all conditons if and only if the polynomial represented in (9) is stable.

### 3.3 Controller Design for MIMO plant

Figure 2 displays the 2-DOF PIDF controller structure of MIMO plant using the proposed method in which independent controllers are formulated for each loop of the MIMO system. The edge theorem is employed to get the robust values of PIDF controller. The design steps for the design of controller for MIMO system $G(s)$ are as follows:

**Step 1:** Initially, the individual transfer function of the given transfer matrix is identified for which controller is designed and the closed-loop characteristic equation, $G_c(s)$ is written for each loop of the MIMO plant for which controller is designed.
**Step 2:** Substitute $s = j\omega$ in the characteristic equation $G_c(s)$ and divide into two parts known as real and imaginary.
**Step 3:** To find the range of the controller parameters $K_p$, $K_i$ and $K_d$, one parameter is first assumed, and the other two parameters are determined by solving two resultant equations obtained in previous step. Select the suitable filter coefficient as constant depending on time domain performance under the condition $\omega \geq \omega_{gc}$. $\omega_{gc}$ is the gain crossover frequency of the decoupled plant.
**Step 4:** The lower and upper values of $K_p$, $K_i$ and $K_d$ are placed in the polynomials expressed by Equation (9) to test that obtained gain value is robust stable or not.
**Step 5:** Finally, from the obtained range of the controller parameters, one gain value of the controller parameter is obtained through PSO algorithm.

#### *3.3.1 Controller Design for TRMS*

With the obtained dimension of controller gains of PIDF, the transfer function of main rotor is written as

$$G_{11}(s) = \frac{1.246}{s^3 + 0.9215s^2 + 4.77s + 3.918} \tag{10}$$

The corresponding feedback expression is determined as shown in Figure 2. In the design of a practical controller with derivative action, a high frequency measurement noise will be generated which in turns control signal variations very high. The implication of unwanted signals is minimized by selecting $N$ as described in Equation (4). The location of the filter's pole in the derivative action, which lowers the controller's sensitivity and increases its robust performance in the presence of high frequency is used to determines the value of $N$. The load disturbance rejection performance is improved by using a proper $N$. In this work the values of $N$ is found as 2.9 for main rotor and 5 for tail rotor.

$$s^5 + 3.82s^4 + 7.44s^3 + s^2[17.75 + 1.246K_d] + s[11.36 + 1.246K_p] + 1.246K_i = 0 \tag{11}$$

If $G(s)$ is plant and $C(s)$ is controller's transfer function, the open loop compensated transfer function can be written as $G_0(s) = G(s)C(s)$. Substituting the value of $s = j\omega$, one can represent it as $G(j\omega)C(j\omega) = \alpha e^{j\beta}$, where $|G(j\omega)C(j\omega)| = \alpha$ and $\angle G(j\omega)C(j\omega) = \beta$. The formulated characteristic equation can be represented as [12],

$$1 + \frac{1}{\alpha} e^{-j(180+\beta_i)} G(j\omega)C(j\omega) = 0$$

$$\Rightarrow 1 + Ae^{-j\gamma}G(j\omega)C(j\omega) = 0 \quad (12)$$

$$s^5 + 3.82s^4 + 7.44s^3 + 17.75s^2 + 11.36s + [1.246K_i + 1.246K_p s + 1.246K_d s^2][A\cos\gamma - jA\sin\gamma] = 0 \quad (13)$$

Then substituting the value of $s = j\omega$ gives

$$j\omega^5 + 3.82\omega^4 - j7.44\omega^3 - 17.75\omega^2 + j11.36\omega + 1.246K_i A\cos\gamma + j\omega 1.246K_p A\cos\gamma - \omega^2 1.246K_d A\cos\gamma - j1.246K_i A\sin\gamma + \omega 1.246K_p A\sin\gamma + j\omega^3 1.246K_d A\sin\gamma] = 0 \quad (14)$$

After equating real and imaginary parts to zero, one can get two expressions as

$$j\omega^5 - j7.44\omega^3 + j11.36\omega + j1.246K_p A\cos\gamma\,\omega - j1.246K_i A\sin\gamma + j1.246K_d A\sin\gamma\,\omega^3 = 0 \quad (15)$$

$$3.82\omega - 17.75\omega^2 + 1.246K_i A\cos\gamma - \omega^2 1.246K_d A\cos\gamma + \omega 1.246K_p A\sin\gamma = 0 \quad (16)$$

where the range of controller gains are $[K_p^{max} \quad K_p^{min}]$, $[K_i^{max} \quad K_i^{min}]$ and $[K_d^{max} \quad K_d^{min}]$ for $K_p$, $K_i$ and $K_d$ respectively. One can easily understand that to find the solution of any equations, the unknowns should be similar to the number of equations but here the number of unknowns is more than the number of equations. Therefore, to get the solutions, one unknown is assumed first, and the other unknowns are determined by solving and satisfying Equations (15) and (16) considering $A = 1$ and $\gamma = 0$ [18,19].

To determine the most appropriate region for a robust controller among three sets of controller gains, a stepwise approach is employed. Initially, each set of controller gains is individually considered. Subsequently the remaining gains are calculated through the solution of equations, leading to the identification of a common region as depicted in Figure 3. In the first phase, the range for $K_p$ is established, with the minimum and maximum values being assumed. Then, using Equations (15) and (16), the values for $K_i$ and $K_d$ are computed and displayed in Figure 3(a). Moving on, the process is repeated with $K_i$ being the variable, and $K_p$ and $K_d$ are derived by solving the same Equations (15) and (16) as shown in Figure 3(b). Lastly, $K_d$ is taken as the initial parameter, and $K_p$ and $K_i$ are determined through the solution of Equations (15) and (16) and portrayed in Figure 3(c). Ultimately, the intersection of these ranges is chosen as the robust region for the controller parameters as shown in Figure 3(d). In this work, controller gain values are calculated for main rotor as $K_p$= [0.1 0.6], $K_i$= [1 16.5] and $K_d$= [0.67 1.2] and for tail rotor as $K_p$= [5.2 10], $K_i$= [1 4] and $K_d$= [0.36 6.47]. The above set of parameters also satisfied the edge theorem robust stability criteria displayed in Equation (9). Hence, it is justified that the obtained range of controller parameter is robust.

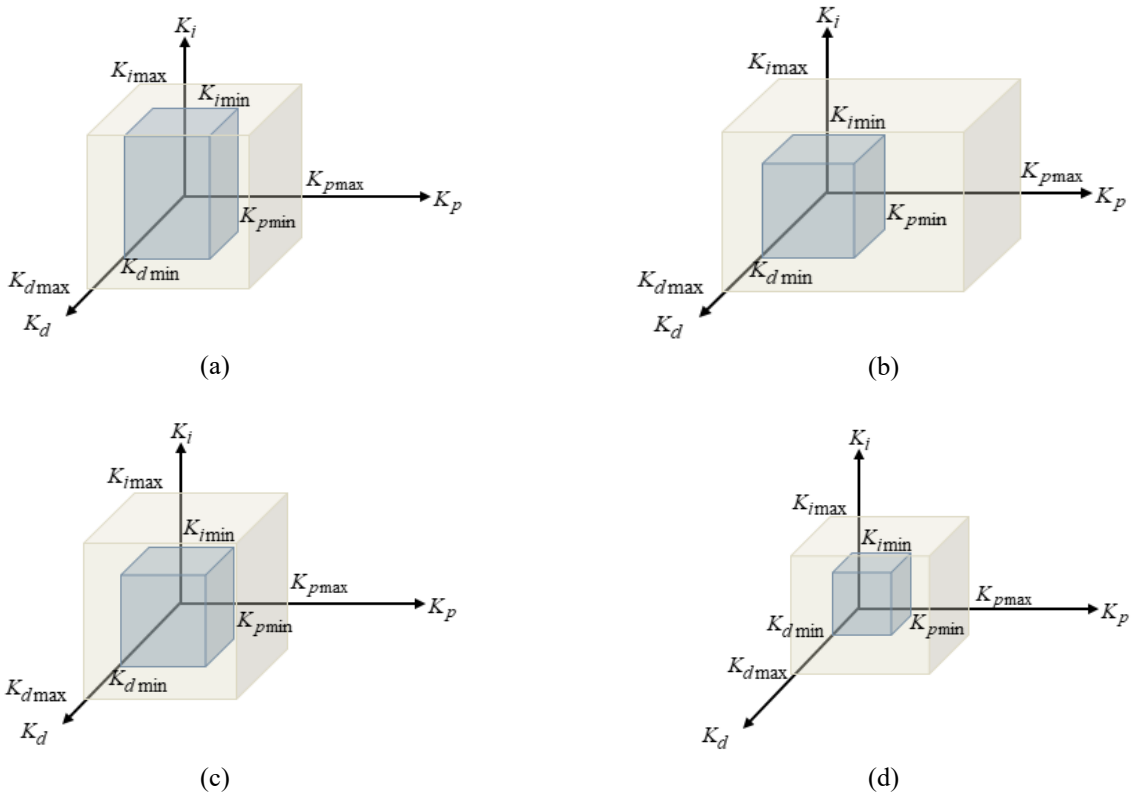


Figure 3. Range of controller gains when (a) $K_p$ is assumed first, (b) $K_i$ is assumed first, (c) $K_d$ is assumed first, (d) Common zone of controller gains.

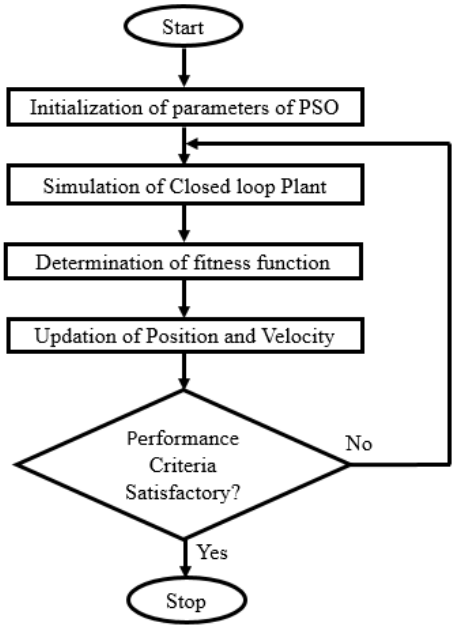


Figure 4. Flow chart of PSO.

### 3.4 Fine Tuning of Parameters Using PSO

Knowing the ranges of controller gains obtained from edge theorem, PSO is satisfactorily applied to tune gains for minimizing fitness function considered here as integral absolute error (IAE) which is described by Equation (17). A population-based stochastic optimization known as PSO is motivated by the social interactions of fish and birds. PSO is a type of evolutionary algorithm that falls under the larger category of algorithms used to solve optimization and search problems. PSO is frequently used to solve a variety of optimization problems in various domains where identifying the best solution is difficult. Its ease of use, effectiveness, and capacity to manage complicated search areas make it a widely used option for optimization. The procedure of PSO algorithm is the combination of initialization where the optimization problem is formulated, and swarms are generated followed by the evaluation of the objective function which is to be minimized. The objective function is minimized by updating the velocity and the positions of the swarms that are initialized until the termination criteria is not satisfied.

$$I.A.E. = \int_0^t \sum_{i=1}^{n} e_i(t)dt \tag{17}$$

where $e$ is the error defined as difference between desired output response and actual output response. In PSO, solution of any problem is represented through the particles. They are represented in $d(1,2,3,\ldots,D)$ dimensional space. Considering $x_i$ is the position of the particle and denoted through $x_i = (x_{i1}, x_{i2}, \ldots, x_{iD})$. $p_{best}$ so far best place according to previous results based on minimum objective function. Out of all that the best position is denoted as $g_{best}$. The optimization algorithm depends upon the velocity of the particle, and it is written by an expression: $v_i = (v_{i1}, v_{i2}, \ldots, v_{iD})$. The velocity of each particle is updated with respect to previous particle following the Equation (18) and known as individual best and among all the particles it is termed as global best. It is mainly dependent on two components called exploration and exploitation which are responsible for motivating the particle to find the search space and guiding the particles towards the best solutions, respectively. Next, each particle's position is updated according to its velocity and current position following Equation (19). Based on the particle fitness values that is to be minimized and which is defined in this problem through Equation (17). The algorithm modifies the global and individual optimum values [13] expressed by Equations (18) and (19).

$$v_{id}^{n+1} = v_{id}^{n} + c_1 rand()(p_{id}^{n} - x_{id}^{n}) + c_2 rand()(p_{gd}^{n} - x_{gd}^{n}) \tag{18}$$

$$x_{id}^{n+1} = x_{id}^{n} + v_{id}^{n+1} \tag{19}$$

where $d$ is the dimension, $v_{id}$ is particle velocity, $c_1$ and $c_2$ are cognitive and group constants, random number is represented as rand (), $x_{id}$ is present situation, $p_{id}$ is best situation, $p_{gd}$ is best position and $n$ is total iteration. The complete process to implement PSO is displayed in Figure 4. Since it is well known the PSO is stochastic approach, therefore in this work, to obtain the guaranteed result the range parameters of the controller which is to be optimized is determined following the procedure of edge theorem described in previous section. It ensures that whatever the value of the controller is obtained through the PSO is surely stabilize the closed-loop compensated system. The population of particles in PSO is one of the important parameters. If its value is large, it allows larger parts of the search space to be covered in one iteration. It results in fewer iterations to reach a good solution compared to smaller population size. The number of iterations is another important aspect of this algorithm depending upon the specific problems if fewer number of iterations is considered it may terminate the search prematurely and a large number of iterations caused unnecessary complex computation. The coefficient $c_1$ and $c_2$ effects on the velocity of the particle and if both values will be zero particles keep flying without updating until it reaches the limit of

search space. If $c_1$ is greater than $c_2$ the method operates as the local search algorithm while if $c_2$ is greater than $c_1$ the entire swarm will move to a particular point only which is also not desirable. Therefore, to get a good balance the most effective approach is $C_1$ should be equal to $C_2$ as stated in numerous cases. Based on all these conditions, values for PSO gains to control TRMS are as follows: Cognitive gain, $c_1 = 1.6$, the group gain, $c_2 = 1.6$, initial population $= 1200$ and iteration number $= 25$.

## 4. SIMULATION RESULTS

By following the proposed procedures described in previous sections, the controller parameters have been determined and the designed controller was tested on TRMS using MATLAB/SIMULINK environment. An input of 1 rad is applied to test the performance of the designed controller. The output responses and the control signals are plotted to investigate the performance of the designed controller.

The results obtained from the simulation are displayed in Figures 5(a) and 5(b), that exhibit step output of both the main and tail rotors. It is worth noting that in these figures, the magnitude of the step response has been set to 1, which is nearly the maximum step response that can be implemented to a given system in real time. The responses unequivocally demonstrate that output effectively tracked the step response in a very short amount of time. Figures 6(a) and 6(b) present control signals for the pitch and yaw angles, correspondingly which also clearly indicate that at no point the control signal crosses the maximum value of the control signal fixed for TRMS which is 2.5 V [1]. The responses have also been utilized to assess the robustness of the developed method. In this evaluation, the main rotor is subjected to the step response, while the tail rotor initially experiences a square signal input. Figure 7 reveals the appropriate output responses that the tail rotor response is square, and the main rotor response is step. The most important thing to be noted is that the square reference tail rotor input does not disturb the performance of the main rotor output. A similar scenario arises when a square input is tested to main rotor and a step signal is applied to tail rotor, as depicted in Figure 8. In this case, the corresponding main rotor response exhibits a square shape, while the yaw angle response follows a step input. One can clearly understand from the transfer matrix of TRMS represented by Equation (3) that a strong coupling effect is present in tail rotor due to main rotor, but the output response of tail rotor is not much disturbed due to the square input applied to main rotor where the output response follows the reference step input only portrayed in Figure 8(b) which clearly indicates the capability of the designed controller.

Furthermore, Table 2 presents a comparison of developed controller implemented plant output responses with the results obtained from earlier investigations available in literature [20]. The data in Table 2 clearly indicates that the developed controller outperforms the preliminary findings. The magnitude of the overshoot and settling time are much lesser in the obtained results as compared to the previous works. The performance of the designed controller is also compared with respect to IAE with the previous work depicted in Table 3 and found that the proposed control method is superior to the previous work [38].

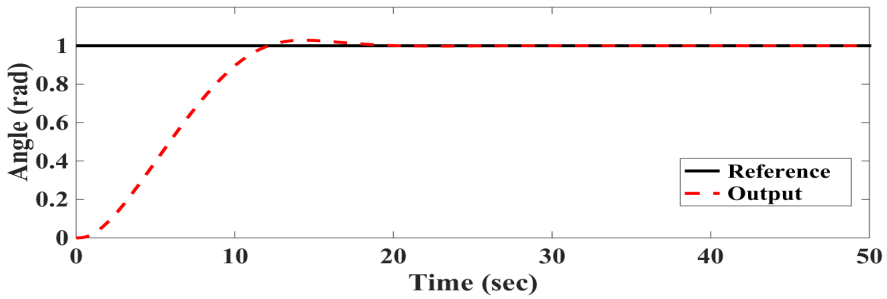


(a)

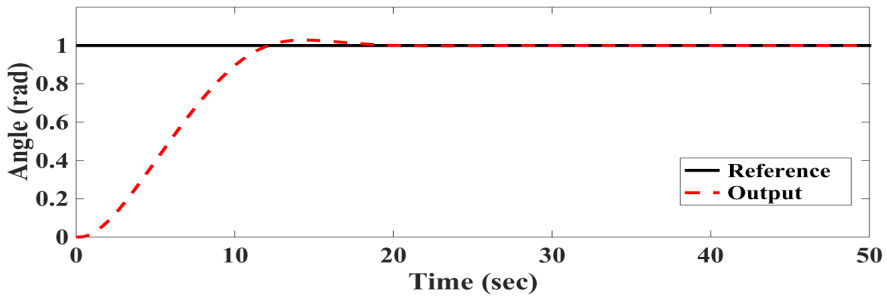


(b)

Figure 5. Output response (a) Main rotor, (b) Tail rotor.

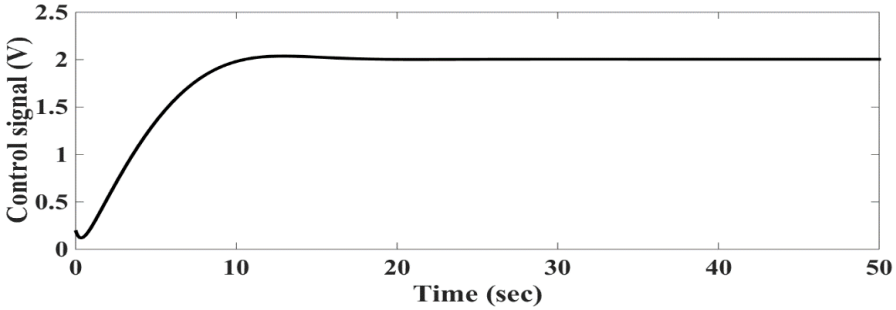


(a)

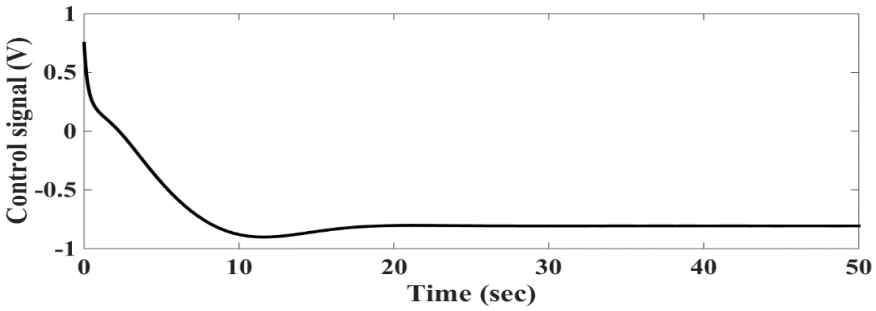


(b)

Figure 6. Control signal (a) Main rotor, (b) Tail rotor.

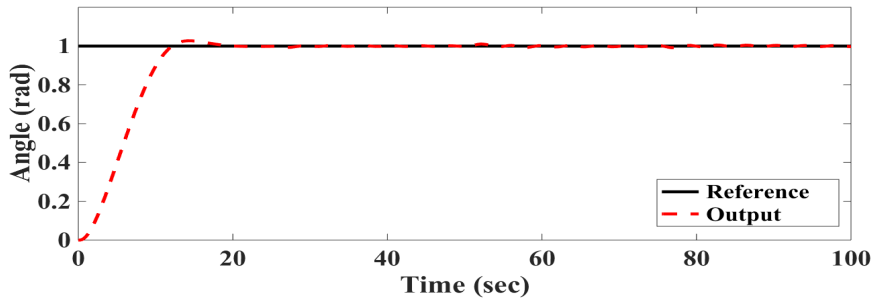


(a)

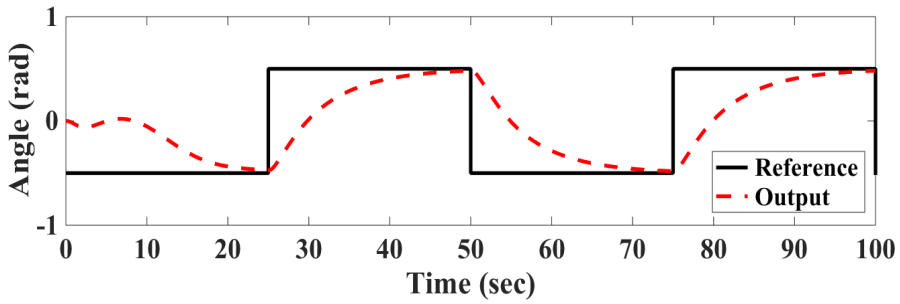


(b)

Figure 7. (a) Main rotor output response for step input when square input is applied to tail rotor, (b) Tail rotor output response for square input.

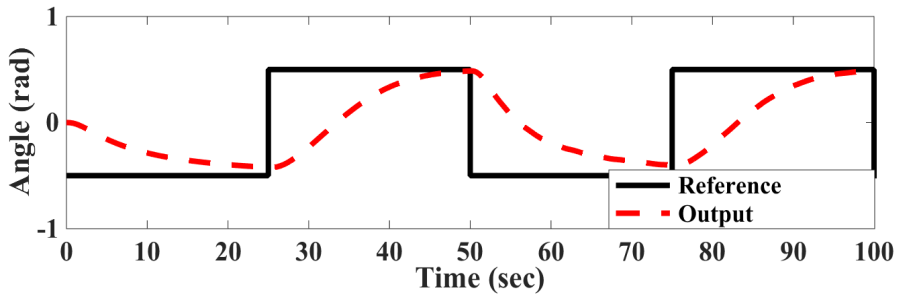


(a)

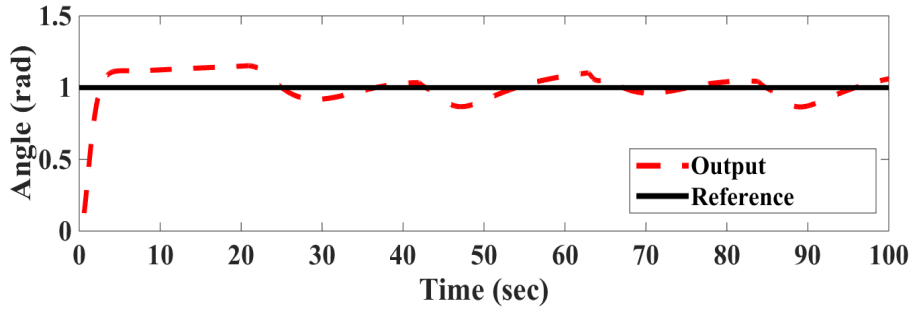


(b)

Figure 8. **(a)** Main rotor output response for square input, (b) Tail rotor output response for step input when square input is applied to main rotor.

Table 2. Comparative study time response performance of TRMS.

| | Vertical plane | | | Horizontal plane | | |
|---|---|---|---|---|---|---|
| | Reference value (rad) | Settling time (sec) | Maximum overshoot (%) | Reference value (rad) | Settling time (sec) | Maximum overshoot (%) |
| Proposed 2-DOF PID controller | 1 | 09 | 0 | 1 | 12 | 8 |
| PSO optimized PID controller [20] | 1 | 20 | 30 | 1 | 10 | 30 |

Table 3. Comparative study of IAE of TRMS.

| | Main rotor | Tail rotor |
|---|---|---|
| Proposed 2-DOF PID controller | 4.1150 | 1.6270 |
| Controller based on chaotic gravitational search algorithm [38] | 10.7582 | 10.7582 |
| Controller based on real coded genetic algorithm [38] | 30.3570 | 30.3570 |

### 4.1 Plant Parameter Variation

The system also exhibits satisfactory performance even when there is a 25% increase in the moment of inertia, which is one of the system parameters. Figures 9(a) and 9(b) depict the output responses of the TRMS when the moment of inertia is increased by 25%.

### 4.2 Disturbance Rejection

The robust performance is also verified by applying output pulse disturbance having the magnitude of 20% to the reference input of the plant. It is applied at time 30 second to main rotor output and removed at 50 second whereas in case of tail rotor output it is applied at time 70 second and removed at 90 second. It is seen from the response plotted in Figure 10 that for both rotors, the designed controller is quite capable of settling the output response within 5 seconds.

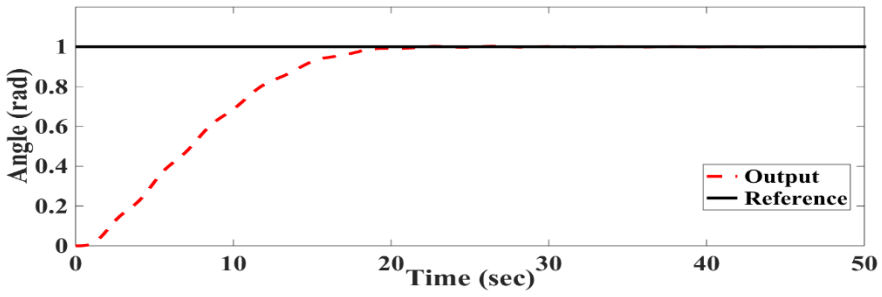


(a)

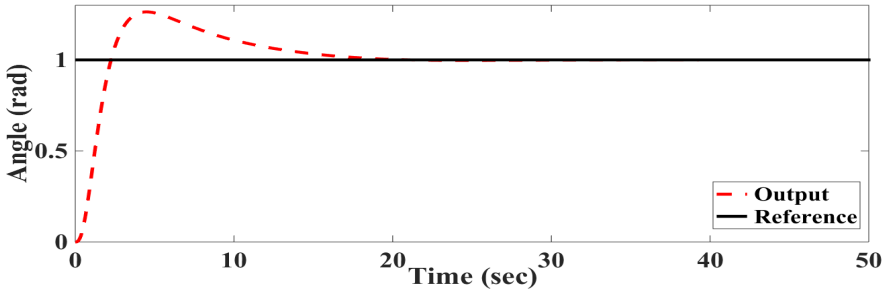


(b)

Figure 9. Step input responses with 25% increment in the moment of inertia of the plant (a) Main rotor, (b) Tail rotor.

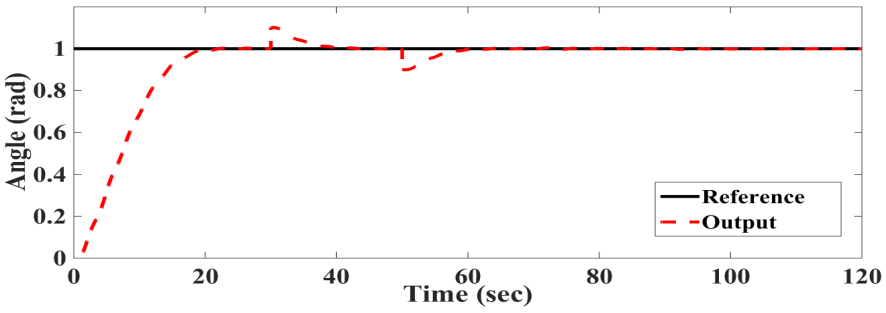


(a)

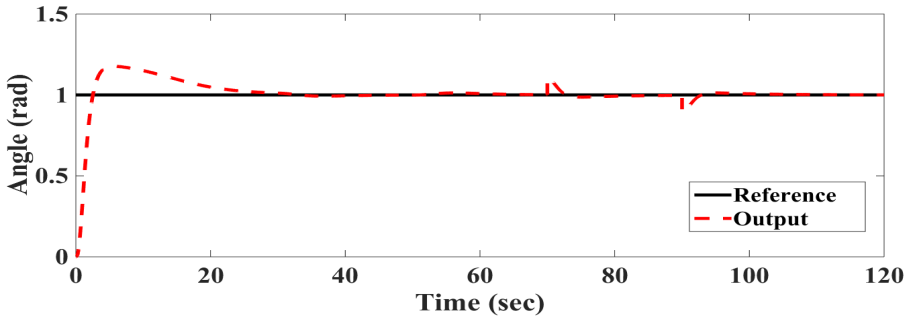


(b)

Figure 10. Output responses in presence of output disturbance (a) Main rotor, (b) Tail rotor.

## 5. CONCLUSION

In this paper, PID based 2-DOF controllers are designed individually for both rotors of TRMS based on edge theorem robust stability criteria. The designed controllers based on edge theorem have been successfully implemented on the non-linear model of TRMS which have a strong coupling effect. The obtained responses indicate that the designed controllers are quite capable of getting the desired performance without incorporating any decoupling scheme. Thus, this control scheme verifies that the application of a decoupler is not necessarily required for TRMS. By altering the reference value's properties, plant parameter variations and output disturbance the designed controller's robust performance is also tested. The effectiveness of this work is also evaluated in comparison to earlier findings. It is evident that the proposed controller delivers notably improved performance compared to the previous results available in literature.

**ACKNOWLEDGEMENT AND FUNDING**

The authors acknowledge all the concerned who support this work. The authors receive no financial support for the research, authorship, and publication of this article.

**DECLARATION OF CONFLICTING INTERESTS**

The authors declare no potential conflicts of interest with respect to the research and publication of this article.

**REFERENCES**

[1] Feedback Instruments Ltd Twin rotor MIMO system, Manual 33-007-0, Sussex, UK. 1996.
[2] S. P. Bhattacharyya, H. Chapellat and L. Keel, *Robust Control: The Parametric Approach*, Prentice-Hall, New Jersey, 1995.
[3] I. M. Horowitz, *Synthesis of Feedback Systems*, Academic Press, 1963.
[4] S. K. Pandey, J. Dey and S. Banerjee, Design of robust proportional – integral - derivative controller for generalized decoupled twin rotor multi-input-multi-output system with actuator non-linearity, *Journal of Systems and Control Engineering*, 232, 2018, 971-982.
[5] S. K Pandey, V. Laxmi, Control of twin rotor MIMO system using PID controller with derivative filter coefficient, *Proceeding of IEEE Student's Conference on Electrical Electronics & Computer Science*, Bhopal, India, 2014, 1-6.
[6] K. L. Chien, J. A. Hrones and J. B. Reswick, On the automatic control of generalized passive systems, *Transactions of the American Society of Mechanical Engineers*, 74, 1952, 175-185.
[7] R. Kuwata, An improved ultimate sensitivity method and PID: characteristics of I-PD control, *Transactions of the Society of Instrument and Control Engineers*, 23, 1973, 232-239.
[8] J. K. Pradhan and A. Ghosh, Design and implementation of decoupled compensation for a twin rotor multiple-input and multiple-output system, *IET Control Theory and Application*, 7(2), 2013, 282-289.
[9] P. Wen and T. W. Lu, Decoupling control of twin rotor MIMO system using robust deadbeat control technique, *IET Control Theory and Application,* 2(11), 2008, 999-1007.
[10] Q. Ahmed, A. I. Bhatti and S. Iqbal, Nonlinear Robust decoupling control design for twin rotor system, *Asian Control Conference*, Hong Kong, China, 2009, 937-942.
[11] H. Ambrose and Z. Qu, Model reference robust control for MIMO systems, *International Journal of Control*, 68(3), 1997, 599-624.
[12] G. Leena and G. Ray, A set of decentralized PID controllers for n-link robot manipulator, *Sadhana*, 37(3), 2012, 405-423.
[13] P. Biswas, R. Maiti, A. Kolay and K. Das, PSO-based PID controller design for twin rotor MIMO system, *International Conference on Control Instrumentation Energy & Communication*, India, 2014, 56-60.
[14] D. K. Saroj, I. Kar and V. K. Pandey, Sliding mode controller design for twin rotor MIMO system with a nonlinear state observer, *International Multi Conference on Automation, Computing, Communication, Control and Compressed Sensing*, India, 2013, 668-673.
[15] J. Lidiya and S. J. Mija, Robust $H_\infty$ control algorithm for twin rotor MIMO system, *IEEE International Conference on Advanced Communication Control and Computing Technologies,* India, 2014, 168-173.
[16] S. M. Ahmad, A. J. Chipperfield and M. O. Tokhi, Dynamic modelling and optimal control of a twin rotor MIMO system, *National Aerospace and Electronics Conference*, Dayton, USA, 2000, 391-398.
[17] A. Ulasyar and H. S. Zad, Robust and optimal model predictive controller design for twin rotor MIMO system, *International Conference on Electrical and Electronics Engineering,* Turkey, 2015, 854-858.
[18] S. K. Pandey, J. Dey and S. Banerjee, Generalized discrete decoupling and control of MIMO systems, *Asian Journal of Control*, 24(6), 2021, 3326-3344.
[19] S. K. Pandey, J. Dey and S. Banerjee, Modified Kharitonov theorem based optimal PID controller design for MIMO systems, *Journal of Electrical Engineering & Technology*, 18, 2022, 2317-2334.
[20] S. K. Pandey, J. Dey and S. Banerjee, Design of optimal PID controller for control of twin rotor MIMO system (TRMS), *Advances in Power and Control Engineering, Lecture Notes in Electrical Engineering*, 609, 2020, 93-106.
[21] A. Haruna, Z. Mohamed, A. M. Abdullahi and M. A. M. Basri, A review of control algorithms for twin rotor systems, *Applications of Modelling and Simulation,* 7, 2023, 93-99.
[22] M. R. Ghazali, M. A. Ahmad and R. M. T. Raja Ismail, Data-driven neuroendocrine PID controller design for twin rotor MIMO system, *Journal of Physics: Conference Series*, 1529, 2020, 1-12.
[23] M. H. Torshizi, H. Rahmani, H. Moeinkhah, M. R. Gharib and J. Jahanpour, A QFT robust controller as a remedy for TRMS, *Aviation*, 24(4), 2020, 137-148.
[24] J. K. Goyal, S. Aggarwal, S. Ghosh, S. Kamal and P. Dworak, Quasi-LPV PI control of TRMS subject to actuator saturation, *IET Control Theory and Applications*, 14(19), 2020, 3157-3167.
[25] T. Dogruer and N. Tan, Decoupling control of a twin rotor MIMO system using optimization method, *International Conference on Electrical and Electronics Engineering*, Turkey, 2019, 780-784.
[26] S. Modak and S. Bhaumik, Comparative study of controllers for twin rotor MIMO system, *International Conference on Computer, Electrical & Communication Engineering (ICCECE)*, Kolkata, India, 2020, 1-6.
[27] S. K. Pandey, J. Dey and S. Banerjee, Internal model control (IMC) of MIMO systems, *IETE Journal of Research*, 69 (7), 2023, 4360-4377.

[28] S. K. Pandey, J. Dey and S. Banerjee, Generalized decoupling and robust control of unstable MIMO system, *Advances in Power and Control Engineering (Lecture Notes in Electrical Engineering)*, 609, 2019, 13-23.
[29] H. Shibly and O. H. Shibly, Formulation method of gain calculation at marginal stability of a linear invariant control systems, *Applications of Modelling and Simulation*, 7, 2023, 16-28.
[30] M. I. Faruk, S. S. Farinwata and A. M. Abdullahi, Modelling and PID control of an in-wheel motor, *Applications of Modelling and Simulation*, 2(3), 2018, 107-113.
[31] K. Aseem and S. Selva, Closed loop control of DC-DC converters using PID and FOPID controllers, *International Journal of Power Electronics and Drive System*, 11(3), 2020, 1323-1332.
[32] S. Vivek, B Varsha, S. T. Vignesh, K Anirudh and K. P. Peeyush, Design of control systems for ABC and speed control for autonomous vehicle, *Journal of Physics: Conference Series,* 1706, 2020, 1-8.
[33] S. Selva Kumar and S. Balamurugan, Common error reference based parallel operation of gas turbine plants, *IEEE International Conference on Intelligent Computing, Instrumentation and Control Technologies*, India, 2017.
[34] A. Chatterjee and K. P. Peeyush, Design of control system for autonomous harvester based on navigation inputs, *Advances in Electrical and Computer Technologies,* 672, 2020, 1129-1137.
[35] S. K. Pandey, J. Dey and S. Banerjee, Design of two DOF PID controller based on Kharitonov's stability theorem for control of TRMS, *International Journal of Mechanical and Production Engineering Research and Development*, 2018, 140-147.
[36] A. Sideris and B. R. Barmish, An edge theorem for polytopes of polynomials which can drop in degree, *Systems & Control Letters,* 13(3), 1989, 233-238.
[37] M. Fu, A. W. Olbrot and M. P. Polis, Robust stability for time-delay systems: The edge theorem and graphical tests, *IEEE Transactions on Automatic Control*, 34(8), 1989, 813-820.
[38] M. W. Iruthayarajan, S. G. Prasad, S. Abishek and P. Vignesh, Choatic GSA based design of multivariable centralised fractional-order PID controller for TRMS, *Global Conference for Advancement in Technology (GCAT), Bangalore, India*, 2019, 1- 4.